Construction and Building Materials, vol. 118 (2016), pp. 1-10.
http://dx.doi.org/10.1016/j.conbuildmat.2016.05.045

Development of an estimative model for the optimal tack coat dosage based on aggregate gradation of hot mix asphalt pavements

A.C. Raposeiras [a]*, J. Rojas-Mora [b, c], E. Piffaut [a], D. Movilla-Quesada [a], D. Castro-Fresno [d]
[a] *Civil Engineering Institute, Austral University of Chile, Valdivia, Chile*
[b] *Statistics Institute, Austral University of Chile, Valdivia, Chile*
[c] *School of informatics, Universidad Católica de Temuco, Temuco, Chile*
[d] *School of Engineering, University of Cantabria, Santander, 39005 Santander, Spain*

ABSTRACT
In this work the performance of tack coats on asphalt pavement layers is analysed. Adjustment models based on experimental measurements were implemented, relating surface layer macro-texture and aggregate content larger than 8 mm. The best fits were obtained with a Gompertz model, which follows the expected physical macro-texture changes outside the test range. Shear strength was analysed, through prediction curves of each evaluated tack coat dosage, with an optimum tack coat performance for aggregate contents larger than 8 mm between 45% and 50%, and no relevant influence of the tack coat dosage used.
Keywords: *Tack coat; Aggregate gradation; Macro-texture; Optimal dosage; Shear strength*

1. Introduction

Deteriorations appear frequently on flexible pavements due to slippage of their layers, especially in areas of acceleration or deceleration, crosses or curves. In these areas, the critical stress level is located at the interface of the upper layers (base/binder and surface layers), whereby the level of bonding between them directly affects the performance and serviceability of the pavement. This bond is ensured by extending asphalt emulsions, as tack coats. The use of such coats as a bond improvement method has been supported by several authors [1, 2, 3], who showed that its use significantly increases the lifetime of a flexible pavement, avoiding premature failures due to slippages, or fatigue failures in areas of high intensity loads generated in the horizontal direction. Mohammad et al. [4] conclude that the importance of such coats increases for thinner pavement layers, especially in the upper layers.

Studies related to implementing tack coats have focused on understanding the main parameters inherent to emulsion characteristics, which have a direct influence on the bond degree achieved by the coat. These parameters include the type of emulsion used, dosage applied, binder-aggregate adhesion in the interface or setting time of the emulsion [4, 5, 6, 7, 8, 9, 10, 11, 12]. Some authors have further evaluated the importance of surface conditions on pavements, such as the degree of surface dust particles or the level of surface texture, which highly influences the final bond degree between layers, in some cases more than the characteristics of the emulsion [2, 8, 11, 13]. Raposeiras et al. [8] indicate that the surface macro-texture of the layer influences slippage resistance between pavement layers bonded by a tack coat. This knowledge is fundamental when selecting an adequate emulsion dosage for the coat.

A procedure for estimating the strength range generated by the tack coat prior to its application, based on the results of the surface characteristics is yet to be implemented, allowing the selection of the optimal emulsion dosage. A model using experimental data from shear strength tests was adjusted, which allows us to estimate the optimal magnitude of slip resistance on layer interfaces before the tack coat is applied. This is analysed according to the aggregate gradation of the asphalt layer to which the tack coat is applied, which is directly related to the macro-texture degree of the asphalt layer [8].

2. Background

2.1. Influential factors on the bond between layers

It is well known that bonding between layers depends on several factors [1, 5, 14, 15]. One of the most studied factors is the applied binder dosage. In terms of residual binder dosage, Collop et al. [14] obtained that the best results are achieved with low dosages, in contrast to what was observed by Recasens et al. [7] and Raposeiras et al. [8], who obtained the least effective dosages below 300 g/m2 of residual binder and the best results from 300 to 450 g/m2.

Chen et al. [5] and Deysarkar [6] studied the emulsion setting time and found that shear strength decreases when the surface layer is extended prior to emulsion breaking. However, Tashman et al. [11] point out that this effect has minimal influence on the magnitude of strength. As for the type of emulsion, Mohammad et al. [9] and Zamora-Barraza et al. [12] concluded that this factor influences tack coat performance since higher strength values are obtained with modified and trackless emulsions than those produced by conventional emulsions. Many of the authors mentioned above indicate that there must be external factors more influence on the final strength other than the type and dosage of binder.

This has led to the study of the role of layer surface condition where the coat is applied. Raab & Partl [2, 16] evaluated the effect of surface pollutants, such as water or dust, concluding that the presence of these agents significantly decreases shear strength, with a more pronounced effect in low emulsion dosages.

Another important factor is the surface finish, which was evaluated by Tashman et al. [11], who observed greatest sample strength with milled surfaces, where the tack coat has a minimal influence. Raposeiras et al. [8] evaluated the role of the surface layer macro-texture to where the coat was applied. This parameter is defined as the degree of surface deviations present in the longitudinal direction range of 0.5 to 50 mm and peak amplitude of 0.2 to 10 mm, in relation to a flat surface [17]. The influence of this variable was estimated, observing that the greatest shear strength results are generated for high macro-texture values, while the lowest ones are observed for lower macro-texture values and also sawn surfaces. This study also shows that there is not an optimum tack coat dosage value valid for all types of asphalt mixes, but that this depends directly on the layer macro-texture.

2.2. Assessment and prediction of the macro-texture of asphalt mixes

Currently there are two types of procedures to assess macro-texture of an asphalt mix layer. The first one is the volumetric method or sand patch test (ASTM E965-06 [18] and UNE-EN 13036-1:2010 [19]), in which glass spheres, with specified sizes between 0.18 mm to 0.25 mm, or sand, with particles between 0.16 mm and 0.32 mm or between 0.16 mm and 0.08 mm, are used as a means to determine surface voids through Mean Texture Depth (MTD). On the other hand, methods based on longitudinal profiles use instruments with laser technology to measure the Mean Profile Depth (MPD), as specified by the ASTM E1845-09 [20] standard, which is then linearly transformed to values that are equivalent to the Mean Texture Depth (MTD).

In order to predict macro-texture levels of an asphalt pavement, Stroup et al. [21] developed a mathematical model based on characteristics of the aggregate mix. The adjusted values were obtained from measurements of samples from 20 different US roads with Superpave, SMA (Stone Mastic Asphalt) and OGFC (Open Graded Friction Courses) mixes. The model used consists of a linear combination of four variables defined from the aggregate gradation to determine the Estimated Texture Depth (ETD) [22]:

$$ETD = 0.0198 \cdot MS - 0.004984 \cdot P4.75 + 0.1038 \cdot C_c - 0.004861 \cdot C_u \quad (1)$$

, where: MS corresponds to the maximum nominal diameter of the aggregate, in mm; P4.75 corresponds to the percentage of aggregate passing through a 4.75 mm sieve, in %; Cc corresponds to the coefficient of curvature; and Cu correspond to the coefficient of uniformity.

The coefficients Cc and Cu are defined as:

$$C_c = (D_{30})^2/(D_{10} \cdot D_{60}) \quad (2)$$

$$C_u = D_{60}/D_{10} \quad (3)$$

, where: D_{10} corresponds to the sieve size associated to 10% passing, in mm; D_{30} corresponds to the sieve size associated to 30% passing, in mm; and D_{60} corresponds to the sieve size associated to 60% passing, in mm.

From the analysis of the model´s variables (1) it is observed that the maximum aggregate size MS is the indicator with the largest influence on macro-texture values estimated by the model. However, for this to be truly representative, the percentage of MS from the total aggregate mass must be considered, that is the probability of this aggregate to be present on the surface. The percentage of aggregate passing through the 4.75 mm sieve is a measure to quantify aggregates of smaller diameter filling surface voids generated by higher aggregates and to a certain degree reducing surface macro-texture. This effect is also dependent on the compaction level of the mixture. Curvature and uniformity coefficients are indicators of the aggregates' distribution degree, and they are used in the model to represent variability in the observed textures of SMA and OGFC mixes, with a non-uniform distribution of their gradation.

The model showed a relatively low correlation level, with a coefficient of determination R2 = 0.65, which may be attributed to the fact that their influence would not be represented by a linear model, or that there are important variables not included in the model. Another important factor to consider is the mixture's variations in void content. Results show that the best fits are obtained for mixes of uniform gradation with relatively similar void content. Another key characteristic is the wear level in the rolling surface for the analysed tracks, since it causes a significant variation on measurements [23].

Prowell & Hanson [23] obtained another model for rolling surfaces based on test track samples under normal traffic conditions. The fineness modulus (FM) variable was considered to represent the aggregates influence , which is estimated as the sum of the retained cumulative aggregate percentages in standard sieves of 0.15 mm, 0.3 mm, 0.6 mm, 1.18 mm, 2.36 mm, 4.75 mm, 9.5 mm, 19 mm, 37.5 mm, 75 mm, 150 mm and dividing this value by 100. This variable influences aggregate size proportional to their diameter and relative quantity on the total whole aggregate. Superpave and SMA mixes were considered for a first estimate, where macrotexture measurements were obtained from sand patch tests, in which the Mean Texture Depth (MTD) and the fineness module (FM) are related by means of a quadratic polynomial:

$$MTD = 0.6421 \cdot FM^2 - 5.235 \cdot FM + 11.224 \quad (4)$$

With a coefficient of determination R2 = 0.62, this model could still be improved. This is attributed to the overestimation of the influence of large diameters in the gradation configuration due to the FM. They do not constitute a significant proportion in relation to total aggregate mass, which, given the mechanics of the compaction process, are decanted mostly to the bottom of the asphalt layer [24]. This is particularly noticeable for gradations with uniform aggregate distributions, as shown in the results section.

Prowell & Hanson [23] evaluated a second model that included OGFC mixture types, measured with a circular texture meter (laser device), obtaining an improved fit, in this case for the Mean Profile Depth (MPD) with R2 = 0.84:

$$MPD = 0.4973 * FM^2 - 3.926 * FM + 8.287 \quad (5)$$

This improvement is attributed to the use of mixes with non-uniform gradations, in which high values produced by the model are balanced with the increased presence of voids in OGFC mixes, which in turn generates an increase in the surface layer macro-texture. The surface wear, due to road traffic, distorted macro-texture values to an appreciable extent, which varied between different sections of the road.

The models discussed above present problems when fitting mixes of uniform gradations. The variables used to represent aggregate influence on macro-texture fail to satisfactorily explain their distribution on the asphalt surface layer. The distribution effect of large aggregate particles is not considered in the representation of surface surface voids produced by the maximum diameter of the aggregates in each configuration, in which the proportion of total aggregates is very low. Therefore, uniform gradation requires the use of a variable that considers the fraction of maximum size aggregates and also extends to larger and intermediate sizes, which also have a significant influence on texture. Surface wear is not an influential factor for this study since the model applies only to intermediate layers, in which wear and loss of texture does not occur with use.

3. Test methodology

For macro-texture measurements, Marshall samples of hot-mix asphalt, 65 mm thick and 101.6 mm in diameter, were prepared according to Marshall design method. Asphalt cement type B50/70 and ophitic type aggregates were used, with no more than 5% of binder in the mixture, depending on the results of optimal binder percentage according to Marshall's design. In order to evaluate different values of macro-texture, 7 types of gradation were selected; 24 samples were prepared per gradation. The aggregate content for each mixture type is set as indicated in the PG-3 [25] for asphalt mixes of continuous gradation of dense, semi-dense and coarse aggregate types. Selected mixes correspond to AC16D, AC22D, AC16S, AC22S, AC22G, AC32G and AC22G (M) whose gradations are indicated in Fig. 1.

The macro-texture measurement was performed through a volumetric method (Fig. 2), similar to the sand patch test defined in UNE-EN 13036-1:2010 standard [19], with the difference that it is applied in to smaller scale samples where macro-texture depth (H) is estimated as:

$$H = \frac{V_m}{A_c} \tag{6}$$

, where: V_m corresponds to the volume of material used to fully screed the surface; A_c corresponds to the area on which it is applied.

An ophitic filler was used, with the characteristics specified in Table 1. It has a smaller particle size than regular sand, indicated in the standard, helping to adapt to surface texture of the mixture. It has a higher percentage of voids and a lower density than common sands, which provides a better compaction effect allowing surface deviations to be fulfilled, obtaining accurate values, particularly in layers with low macro-texture depths.

The measured values were then standardized, by correcting the results through:

$$Mn = Mf * 1.271 + 0.041 \tag{7}$$

This model correlates measured macro-texture values with the ophitic filler (Mf) using values obtained for a standard sand with particle sizes between 0.16 mm and 0.32 mm (Mn).

Macro-texture values obtained from the test are shown in Table 2, together with the statistical parameters for each type of asphalt mixture. Macro-texture clearly increases with the content of coarse aggregates, having the opposite effect for the fine aggregate proportion, indicating that less closed gradations generate higher macro-texture values.

4. Estimated macro-texture model based on aggregate gradation

According to the test results the lower macro-textures correspond to AC16D, AC16S and AC22D asphalt mixes, containing similar magnitudes, which can be traced back to their low content of coarse aggregates. It is also noted that the increase in maximum particle size between AC16D and AC22D mixes do not produce an increase in macro-texture as one might expect; this phenomenon is related to the compaction process [24].

During this process aggregates with smaller sizes tend to deposit heavily on the surface, due to their high ratio relative to the total aggregate mass. On the other hand, due to the lower ratio of larger particles these tend to remain at the bottom and middle of the asphalt layer thereby generating a low impact on surface deviation.

Although AC22D, AC22S, AC22G (M) and AC22G mixes have the same maximum particle size, different textures values are observed. This indicates that variations of intermediate particle quantities for each configuration have a high influence on sample surface deviations, when the percentage from total aggregate is increased, due to the distribution effect produced by compaction of the asphalt layer. This is observed in AC22G and AC32G mixes, where the maximum particle size increases considerably but the macro-texture variation is maintained within a similar range to the previous mixes. For uniform particle size gradations, not only particles of maximum aggregate size influence macro-texture, but the intermediate fraction is also important due to its large proportion in the mixture and also for its effect on the compaction process.

According to this result, a size limit exists, beyond which aggregates considerably influence texture. The macro-texture measured in the test is evaluated in relation to aggregate percentages retained by sieves of 2, 4, 8 and 16 mm, (Fig. 3). A clear trend in macro-texture measurements is observed in sieves over the size of 8 mm (Fig. 3(b)), presenting a proportional relationship between variables. The variables of the lower sizes of 2 and 4 mm (Fig. 3(c) and Fig. 3(d)) have no clear correlation with the AC16D and AC16S mixes. The 16 mm size did not accurately explain deviations in mix texture (Fig. 3(a)) because it does not consider the high proportion of intermediate size aggregates. Therefore, the 8 mm size is considered the representative value of the aggregates influence on macro-texture.

The percentage of aggregates larger than 8 mm in each type of asphalt mixture tested is shown in Table 3. When analyzing macro-texture in relation to the percentage of aggregates larger than 8 mm (Fig. 3(c)), it can be observed that mixes under 40% have similar textures, with low variations between them, caused by the high content of fine aggregates and the low amount of coarse aggregates on the surface layer. The surface deviations produced by coarse aggregates are mostly covered by the fine aggregates. It was observed that increases of this variable has an important effect on macro-texture with an almost linear relationship between these variables when the percentage of aggregates larger than 8 mm is over 40%. This indicates that the volume of particles larger than 8 mm is distributed in the layer surface, producing larger surface deviations. These deviations fail to be covered by fine aggregates since these reduce their proportion when the amount of coarse aggregate increases.

The data was fitted to three mathematical models using ordinary least squares (OLS): the first one corresponds to the modified Gompertz model with a linear component (8); the second to a cubic polynomial (9); and the third to an exponential model (10):

$$ETD = a_1 * e^{\left(-a_2 * e^{\left(-a_3 * G\right)}\right)} + a_4 * G \quad (8)$$

$$ETD = a_1 * G^3 + a_2 * G^2 + a_3 * G + 0.069 \quad (9)$$

$$ETD = \frac{1}{a_1 + e^{(a_2 + a_3 * G)}} + 0.069 \quad (10)$$

, where: ETD is the estimated macro-texture depth in millimeters; and G is the aggregate content greater than 8 mm.

A minimum macro-texture value of 0.069 mm is defined in the models, as this is the value of a layer with sawn surface, and is equivalent to the lower macro-texture achievable by the applied method.

The equations parameters and p-values are defined in Tables 4, 5 and 6. All parameters are considered significant when levels of significance are less than 0.5%.

As a comparative measure of goodness of fit for the models, the value of the Root Mean Square Error (RMSE) for each case is estimated. This is calculated as:

$$RMSE = \sqrt{\frac{\sum_{t=1}^{n}(y_t - \hat{y}_t)^2}{v}} \quad (11)$$

, where: n is the number of observations; yt is the measured experimental value for the i-th observation; ŷt is the models estimated value for the i-th observation; and v is the number of observations minus the number of parameters fitted in the model.

From Table 7 it can be concluded that the modified Gompertz model, although complex, is the best fit for the data. It can be seen in Fig. 4 that the modified Gompertz model fits the data well, especially at contents values smaller than 40%. From this value, the function tends to be more pronounced, presenting an almost linear growth that tends to decay after the 55% mark.

This model shows the low variation of macro-texture attributed to the content range lower than 30%, unlike the polynomial model where the values tend to fluctuate, and the exponential model that underfits the data. The Gompertz model is the only model that captures the expected saturation on macro-texture. This effect is caused by the increased percentage of intermediate aggregates, which maintain their ratio on the surface, when the larger diameter aggregates proportion also increases.

In Fig. 5, residuals for the modified Gompertz model are shown. They are small in relation to the magnitude of the measurements, with a maximum value of about 0.05 mm, demonstrating that the model fits well to the data. They are randomly distributed around the origin, implying the absence of a clear autocorrelation. Similarly, Fig. 6 shows residuals in a standardized way. It is observed that the amount of standardized residuals beyond two standard deviations does not exceed 5% of the total value. There are no standardized residuals beyond three standard deviations. Fig. 7 shows the QQ plot of the models standardized residuals against a standardized normal distribution. The results show that the standardized residuals for all cases closely follow a standardized normal distribution, since they are near the diagonal in this plot, an assumption required in the OLS model.

5. Tack coat performance as a function of emulsion dosage and aggregates gradation

The relationship between macro-texture and percentage of aggregates larger than 8 mm is used to analyze the results of shear strength obtained by Raposeiras et al. [8] of two layers samples of asphalt mixes bonded by tack coat. From these tests a direct relationship can be established between shear strength with a high content of aggregates larger than 8 mm, and the coats effect on different residual binder dosages can be evaluated.

The test performed, using the LCB shear test procedure, considers four different dosages for residual binder consisting of a conventional cationic rapid-setting emulsion (European designation: C60B3). This is a standardized test (NLT-382/08) where a shear strength is applied in the interface of two layers samples in order to obtain the shear bond strength of the tack coat.

The analysed gradations correspond to uniform distributions of aggregate grain size, using AC16D and AC22D asphalt mixes (with an estimated macro-texture of 0.20 mm and 0.27 mm respectively) for top layers, while for bottom layers AC22D (with sawn and unsawn surfaces), AC22S, AC22G (M), AC22G and AC32G asphalt mixes were used. Sawn condition is generated using a circular saw, and unsawn condition is the standard surface texture of an asphalt mixture, with no treatment.

AC22D asphalt mixture with a sawn surface corresponds to the lowest macro-texture value measurable through the used volumetric method, a hypothetical limit attributable to a theoretical 0% content of aggregates larger than 8 mm, whose values will be used to represent the lower limit of the gradation variable.

Shear strength values for different mixes, depending on their content of aggregates larger than 8 mm, are represented in Fig. 8. Since influence of asphalt mix top layer type showed to have minimal influence on shear strength according to previous researches [8], all samples have been analysed only based on their bottom layer macrotexture, with no consideration of the top layer mixture type. In the range from 0% to 37.5% shear strength variations are caused by the slight increases in surface texture of the bottom layer, produced by the small increase of coarse aggregate content. Increased deviations provide an increase in shear strength at the interface, due to the friction between the layers, which increases when the content of aggregates larger than 8 mm increases. However, this contribution to interface bonding is not highly significant since the layers are mainly bonded by the action of residual binder tack coat placed on the surface of the bottom layer.

For aggregate larger than 8 mm values higher than 37.5%, significant shear strength variations are obtained as a result of the higher degree of deviations in the bottom layer. This effect is produced by the high surface content of aggregates larger than 8 mm, which create larger contact areas between layers, increasing the shear strength between them. Maximum shear strength is located in the gradation range of 45% to 50%, associated with the coupling between the layers, where it reaches optimum contact area.

For contents higher than 50%, resistance considerably decreases. This can be explained by the large macro-texture present in the bottom layer, compared to the top layer, which produces less friction between layers and therefore reduces the contribution of strength. Also, the amounts of residual binder used are not enough to cover texture deviations in the bottom layer, reducing the bond input of the tack coat.

The curves shown in the graph are models fitted by OLS for each of the dosages tested. These models express resistance (R) for different content percentages of aggregates larger than 8 mm (G), using a Gompertz function with a cubic polynomial component:

$$R = a_1 + a_2 * G - a_3 * G^2 + a_4 * G^3 - a_5 * e^{\left(-a_6 * e^{(-a_7 * G)}\right)} \tag{12}$$

The levels of significance and the parameter values used for each model are shown in Tables 8 to 11. The probability value for the t-statistic indicates that all parameters are significant for all models.

The Root Mean Square Error (RMSE) was calculated for each model, obtaining the values shown in Table 12. The model for the 250 g/m2 dosage presented the worst fit, while the best fit was the 375 g/m2 dosage.

When analyzing the effect of residual binder dosage for each percentage of aggregates larger than 8 mm in the test, it was observed that contents between 37.5% and 42%, corresponding to mixes with low texture depth (Fig. 9(a), Fig. 9(b)), produced the best level of the binder coating from the 375 g/m2 dosage. The application of dosages higher than this value produces an excess of binder between layers, therefore reducing shear strength. Moreover the use of lower dosages fails to efficiently cover the surface, generating a decrease in bonding. However, it was observed that in the dosage of 125 g/m2 shear strength increases. This effect is attributable to the minimum coating binder which produces that deviations between layers remain bounded, producing greater contact at the interface, and thus increasing shear sample strength.

For contents between 45% and 50% of aggregates larger than 8 mm, shear strength is higher for dosages close to 250 g/m2 (Fig. 9(c), Fig. 9(d)). This is because strength is mostly related to the level of contact between layers. Therefore, a large coating binder reduces the shear strength of the union, this effect being appreciable for a dosage of 500 g/m2, where strength is substantially lower than other dosages.

At a level of 55.5% of aggregates larger than 8 mm (Fig. 9(e)), shear strength is again similar for all analyzed dosage levels, explained by the high macro-texture of the bottom layer. This effect indicates that the binder content used is not sufficient to cover the layer and generate a significant level of tack coat binder bonding.

When evaluating both the dosage and percentage of aggregates larger than 8 mm in the models, the greatest difference in shear strength is observed in residual binder dosages between250 g/m2 to 500 g/m2, with a range of 1328 N for 45% of aggregates larger than 8 mm. On the other hand, the maximum difference in shear strength of 4248 N is obtained for aggregate contents larger than 8 mm from 0% to 45% at a dosage of 250 g/m2.

This indicates that shear strength at the interface is influenced more by the distribution of surface aggregates, than the dosage of residual binder applied. The dosage is defined by the degree of contact and friction between the deviations present in both layers, produced by the percentage of aggregates larger than 8 mm.

6. Absorption analysis for the experimental control method of tack dosage as a function of aggregate gradation

The results of the absorption test developed by Raposeiras et al. [8] are assessed for the new experimental dosage control system based on the percentage of aggregates larger than 8 mm and its influence on the device´s degree of absorption.

The device is composed of a steel plate covered with a geotextile, which is responsible for absorbing the binder applied over the layer (Fig. 10). There is a membrane of polyethylene foam that produces an adequate adaptation to the surface and there is also a waterproof polymer sheet to prevent leakage. A constant pressure of 3.14 kPa is maintained for 5 minutes for calibration. The geotextile is then removed and the amount of binder absorbed is determined by comparing geotextile weights before and after the procedure. It is important that measurements are completed immediately after the application of the tack coat (no more than 5 minutes).

The implementation of this device requires previous measurements of the Macro-Texture Depth (MTD) in the layer on which the tack coat is applied. To avoid performing this test in the field, a model is developed that provides an estimation of the absorption percentage required, in terms of the theoretical dosage applied and the known aggregate gradation of the mixture, specifically the percentage of aggregates larger than 8 mm. The measurements used to fit the model are obtained from tests conducted by Raposeiras et al. [8], with 3 levels of emulsion dosages -250 g/m2, 375 g/m2 and 500 g/m2- and aggregate contents larger than 8 mm between 40% to 53%.

In Fig. 11 the measured test values are presented as a function of the proportion of aggregates larger than 8 mm for each dosage analyzed. In terms of this variable, it is observed that the absorption percentage is distributed similarly for the 375 g/m2 and 500 g/m2 dosages, where binder deposited on the surface is absorbed to a considerable extent. However, for lower dosage of 250 g/m2 performance significantly decreases, an effect associated with the absorption capacity of the geotextile and the amount of tack coat which remains on the surface once the gaps related to the macro-texture have been filled. Additionally, it can be observed that this range difference increased for higher percentages of varying particle size, because when increasing the dosage level, the residual binder percentage that is deposited on the texture peaks also increases.

In terms of the influence of aggregates greater than 8 mm, the fitted curves show a similar absorption behavior to the various provisions in the tested range of aggregate gradations. The highest absorption variations occur for aggregate percentages over 40% and up to 50%. This is due to a greater presence of coarse aggregates in the surface, which lead to significant increases in surface deviations and therefore decrease the amount of tack coat absorbed by the geotextile. For aggregate contents between 0 and 40%, it is observed that absorption starts with an asymptotic behavior, the slope then progressively grows, but at a lower rate than the 40% to 50% range. This behavior is attributed to the relative stability of macro-texture in this range, due to the low amount of surface coarse particles. When aggregates larger than 8 mm reach 60%, geotextile absorption is expected to decay following an asymptotic behavior. This effect is due to high surface deviations caused by the increased amounts of coarse aggregates. The increase in deviations hinders emulsion absorption in the tack coat, allowing the geotextile to only reach emulsions deposited on the most salient aggregates in the layer.

The curves shown in Fig. 11 were fitted for each dosage according to the Gompertz model (13) using OLS, where the emulsion absorbed by the geotextile (A) is expressed in terms of the percentage of aggregates larger than 8 mm (G):

$$A = a_1 * e^{-e^{(a_2 * G + a_3)}} + a_4 \tag{13}$$

The values of the parameters for each dosage are presented in Tables 14, 15 and 16. The t-statistic shows that the parameters are significant for all models.

The Root Mean Square Error (RMSE) was calculated for each model, obtaining the values in Table 17. It is observed that the adjustment is relatively similar for all three dosages.

7. Conclusions

The content of aggregates larger than 8 mm included in the gradation of the asphalt mixture proved to be a good indicator of surface deviations in an asphalt layer with uniform gradations. The modified Gompertz model (8), showed the best goodness of fit and residuals following a normal distribution. Additionally this model seems to follow the expected physical behavior for macro-texture outside the range of experimental measurements.

The content of aggregates larger than 8 mm showed a great influence on shear strength between pavement layers bonded by a tack coat, where the contents with the best performance correspond to values from 45% to 50%, relative to the total mass of aggregates. The adjusted models (12) correctly model the variation of strength observed in the tests.

The residual binder dosage of tack coat proved to be only slightly more relevant for contents above 40%. Given its low impact, it is not possible to fit a model with both variables to strength variation provided by the emulsion dosage.

The aggregates content larger than 8 mm proved to be influential on the degree of absorption of the experimental device which controls the dosage. The largest changes in absorption occur in the range between 40% and 60% due to the effect of aggregate distribution in the asphalt layer, with asymptotic behaviors above and below this range. The Gompertz model (13) was suitable for representing the variation, which tends to decrease for dosages of 375 g/m2 and 500 g/m2.

Acknowledgements

The authors would like to acknowledge the support provided by the Technologic Research Construction Group (GITECO) and the Group of Roads of Santander at Cantabria University for the development of tests and samples. We would also like to thank the company Emilio Bolado S.L. and the Society for the Development of Cantabria Region (SODERCAN) for the material provided, and the DID Research Department from the Austral University of Chile for the support.

References

[1] Diakhaté, M., Millien, A., Petit, C., Phelipot-Mardelé, A., & Pouteau, B. (2011). Experimental investigation of tack coat fatigue performance: Towards an improved lifetime assessment of pavement structure interfaces. Construction and Building Materials, 25(2), 1123-1133. http://dx.doi.org/10.1016/j.conbuildmat.2010.06.064

[2] Raab, C., & Partl, M. (2008). Influence of tack coats on the adhesion properties of asphalt pavements. In: 4th International Gulf Conference on Roads. Doha, QATAR. NOV 10-13, 2008 (pp. 517-527).

[3] Ziari, H., & Khabiri, M. M. (2007). Interface condition influence on prediction of flexible pavement life. Journal of Civil Engineering and Management, 13(1), 71-76. http://dx.doi.org/10.1080/13923730.2007.9636421

[4] Mohammad, L., Hassan, M., & Patel, N. (2011). Effects of shear bond characteristics of tack coats on pavement performance at the interface. Transportation Research Record: Journal of the Transportation Research Board, (2209), 1-8. http://dx.doi.org/10.3141/2209-01

[5] Chen, J. S., & Huang, C. C. (2010). Effect of surface characteristics on bonding properties of bituminous tack coat. Transportation Research Record: Journal of the Transportation Research Board, (2180), 142-149. http://dx.doi.org/10.3141/2180-16

[6] Deysarkar, I. (2004). Test set-up to determine quality of tack coat. University of Texas at El Paso.

[7] Recasens, R., Martínez, A., & Jiménez, F. (2006). Evaluation of effect of heat-adhesive emulsions for tack coats with shear test: from the Road Research Laboratory of Barcelona. Transportation Research Record: Journal of the Transportation Research Board, (1970), 64-70. http://dx.doi.org/10.3141/1970-08

[8] Raposeiras, A. C., Vega-Zamanillo, Á., Calzada-Pérez, M. Á., & Castro-Fresno, D. (2012). Influence of surface macro-texture and binder dosage on the adhesion between bituminous pavement layers. Construction and Building Materials, 28(1), 187-192. http://dx.doi.org/10.1016/j.conbuildmat.2011.08.029
[9] Mohammad, L. N., Bae, A., Elseifi, M. A., Button, J. W., & Scherocman, J. A. (2009). Interface shear strength characteristics of emulsified tack coats. Journal of the Association of Asphalt Paving Technologists, 78.
[10] Mo, L., Huurman, M., Wu, S., & Molenaar, A. A. A. (2009). Ravelling investigation of porous asphalt concrete based on fatigue characteristics of bitumen–stone adhesion and mortar. Materials & Design, 30(1), 170-179. http://dx.doi.org/10.1016/j.matdes.2008.04.031
[11] Tashman, L., Nam, K., Papagiannakis, T., Willoughby, K., Pierce, L., & Baker, T. (2008). Evaluation of construction practices that influence the bond strength at the interface between pavement layers. Journal of Performance of Constructed Facilities, 22(3), 154-161. http://dx.doi.org/10.1061/(ASCE)0887-3828(2008)22:3(154)
[12] Zamora-Barraza, D., Calzada-Peréz, M., Castro-Fresno, D., & Vega-Zamanillo, A. (2010). New procedure for measuring adherence between a geosynthetic material and a bituminous mixture. Geotextiles and Geomembranes, 28(5), 483-489. http://dx.doi.org/10.1016/j.geotexmem.2009.12.010
[13] Zhou, Q., & Xu, Q. (2009). Experimental study of waterproof membranes on concrete deck: interface adhesion under influences of critical factors. Materials & Design, 30(4), 1161-1168. http://dx.doi.org/10.1016/j.matdes.2008.06.023
[14] Collop, A. C., Sutanto, M. H., Airey, G. D., & Elliott, R. C. (2009). Shear bond strength between asphalt layers for laboratory prepared samples and field cores. Construction and Building Materials, 23(6), 2251-2258. http://dx.doi.org/10.1016/j.conbuildmat.2008.11.017
[15] Raposeiras, A. C., Castro-Fresno, D., Vega-Zamanillo, A., & Rodriguez-Hernandez, J. (2013). Test methods and influential factors for analysis of bonding between bituminous pavement layers. Construction and Building Materials, 43, 372-381. http://dx.doi.org/10.1016/j.conbuildmat.2013.02.011
[16] Raab, C., & Partl, M. N. (2004, September). Effect of tack coats on interlayer shear bond of pavements. In Proceedings of the 8th Conference on Asphalt Pavements for Southern Africa (CAPSA'04) (Vol. 12, p. 16).
[17] Fwa, T. F. (Ed.). (2005). The handbook of highway engineering. CRC Press.
[18] ASTM E965-15 (2015). Standard test method for measuring pavement macrotexture depth using a volumetric technique. ASTM International, West Conshohocken, PA, Pennsylvania, USA. http://dx.doi.org/10.1520/E0965-15 , www.astm.org
[19] UNE-EN 13036-1 (2010). Road and airfield surface characteristics - Test methods - Part 1: Measurement of pavement surface macrotexture depth using a volumetric patch technique [Características superficiales de carreteras y aeropuertos. Métodos de ensayo. Parte 1: Medición de la profundidad de la macrotextura superficial del pavimento mediante el método volumétrico]. AENOR Standard.
[20] ASTM E1845-15 (2015). Standard practice for calculating pavement macrotexture Mean Profile Depth. ASTM International, West Conshohocken, PA, Pennsylvania, USA. http://dx.doi.org/10.1520/E1845-15 , www.astm.org
[21] Stroup-Gardiner, M., & Brown, E. R. (2000). Segregation in hot-mix asphalt pavements (No. 441). Transportation Research Board.
[22] Terzaghi, K., Peck, R. B., & Mesri, G. (1996). Soil mechanics in engineering practice. John Wiley & Sons.
[23] Prowell, B., & Hanson, D. (2005). Evaluation of circular texture meter for measuring surface texture of pavements. Transportation Research Record: Journal of the Transportation Research Board, (1929), 88-96. http://dx.doi.org/10.3141/1929-11
[24] Masad, E., Muhunthan, B., Shashidhar, N., & Harman, T. (1999). Internal structure characterization of asphalt concrete using image analysis. Journal of computing in civil engineering. http://dx.doi.org/10.1061/(ASCE)0887-3801(1999)13:2(88)
[25] PG-3 (2013). General technical specification for road and bridge Works. [Pliego de preinscripciones técnicas generales para obras de carreteras y puentes]. General Highway Department, Madrid, Spain.

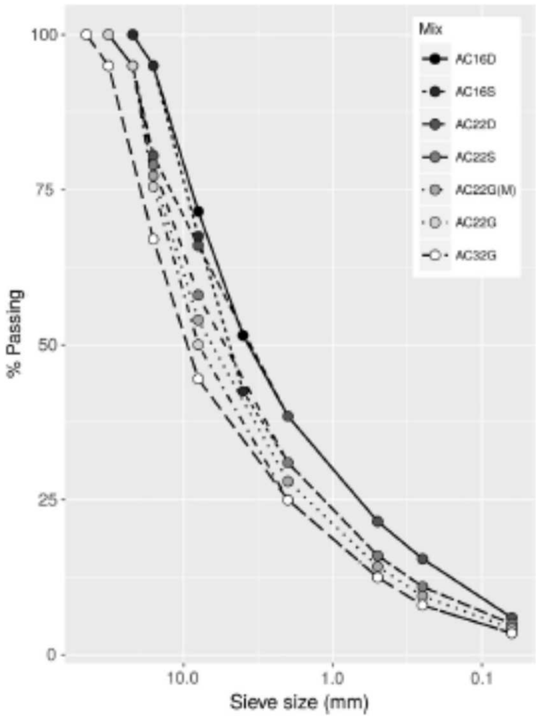

Fig. 1. Hot asphalt mixes gradation analysed.

Fig. 2. Macro-texture measurement methodology.

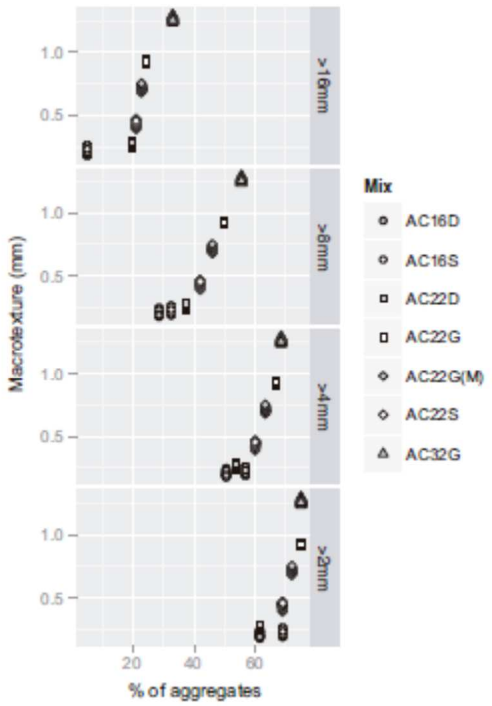

Fig. 3. Macro-texture distribution for percentage of aggregates larger than 16 mm (a), 8 mm (b), 4 mm (c) and 2 mm (d) on the gradations analysed.

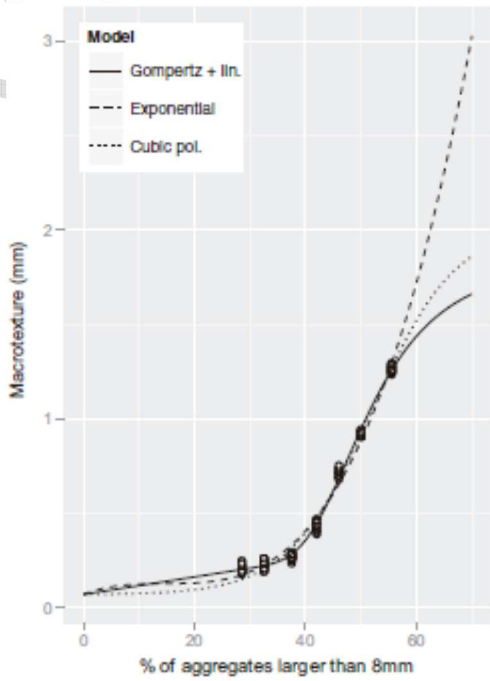

Fig. 4. Macro-texture models distribution.

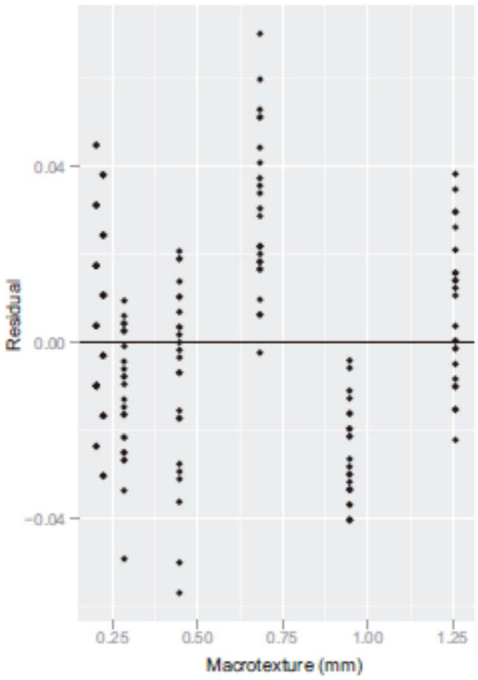

Fig. 5. Residuals for the modified Gompertz model.

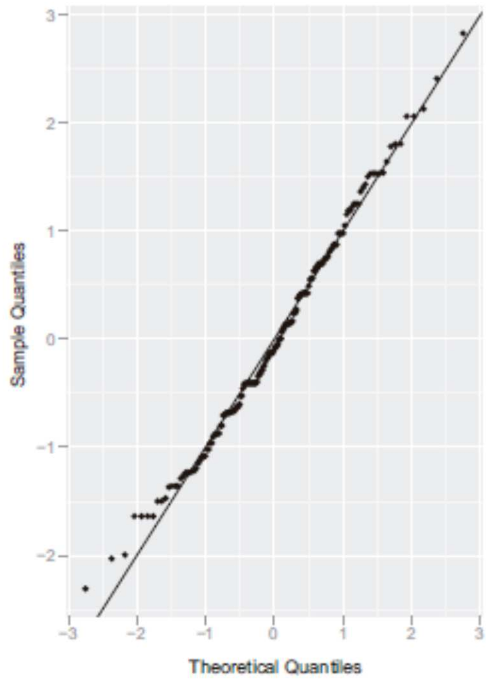

Fig. 7. Q-Q plot of standardized residuals for the modified Gompertz model.

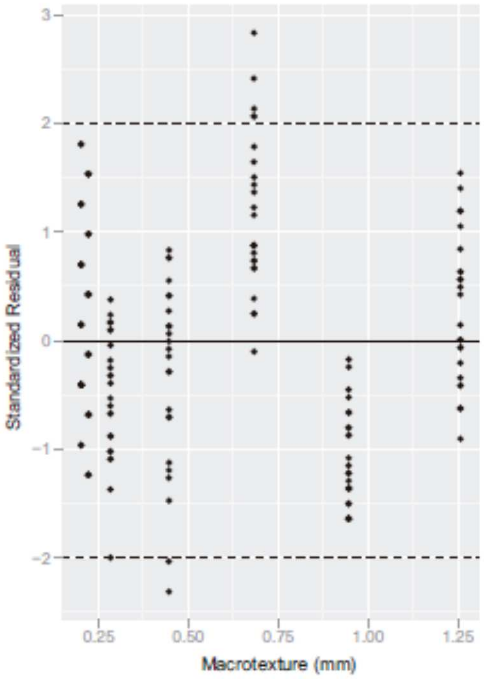

Fig. 6. Standardized residuals for the modified Gompertz model.

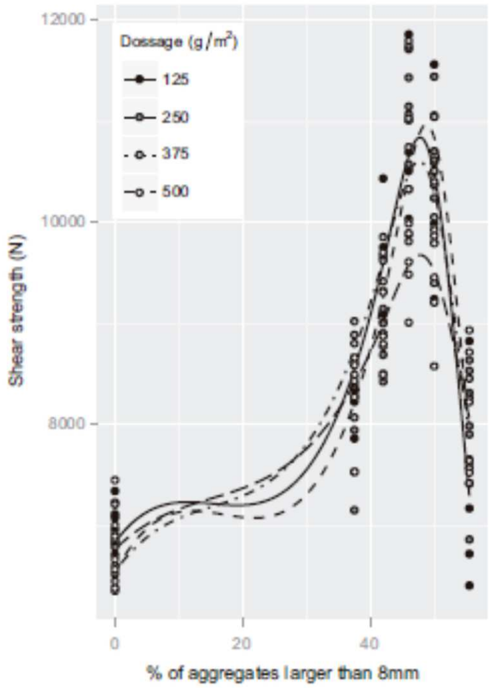

Fig. 8. Shear strength vs. percentage of aggregates larger than 8 mm.

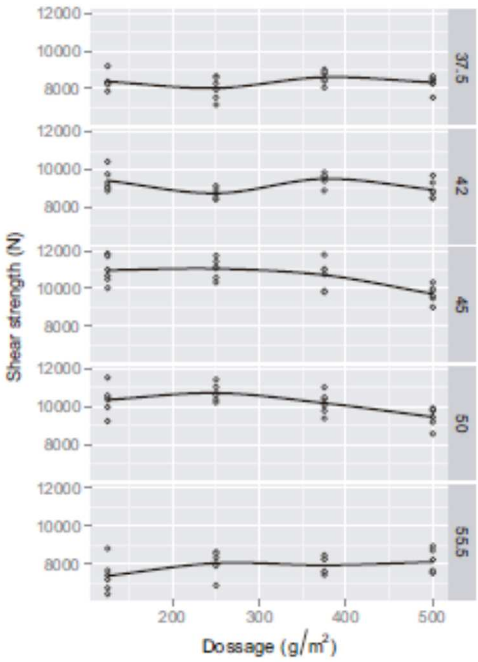

Fig. 9. Shear strength vs. tack coat dosage for gradations with 37.5% (a), 42% (b), 45% (c), 50% (d) and 55.5% (e) of aggregates larger than 8 mm.

Fig. 10. Tack coat dosage control device.

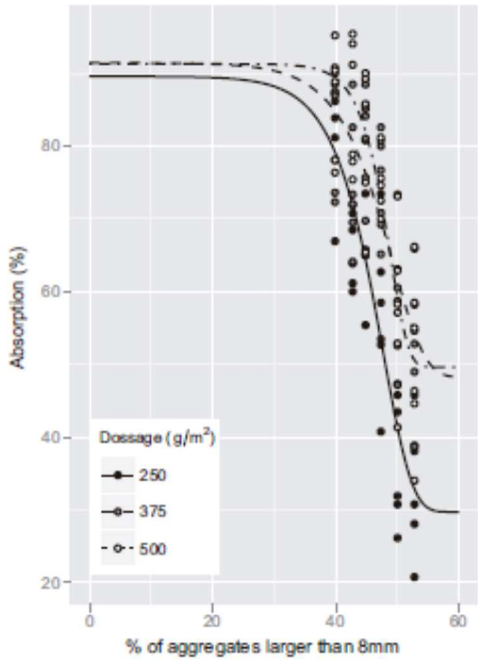

Fig. 11. Absorption for *on site* test vs. percentage of aggregates larger than 8 mm.

Table 1
Characteristics of the ophitic filler used for the measurements.

Particle size [mm]	0.063
Specific gravity [g/cm^3]	2.86
Bulk density [g/cm^3]	0.91
Porosity [%]	68.19

Table 2
Macro-texture test results.

Asphalt mixture type	Mean [mm]	Standard deviation
AC16D	0.206068	0.020509396
AC16S	0.227130	0.022722818
AC22D	0.270702	0.014508894
AC22S	0.437883	0.021528236
AC22G (M)	0.712090	0.018436029
AC22G	0.919899	0.011207113
AC32G	1.264381	0.017003861

Table 3
Average percentage of aggregates retained by a sieve size of 8 mm.

Asphalt mixture type	Aggregates larger than 8 mm [%]
AC16D	28.5
AC16S	32.5
AC22D	37.5
AC22S	42.0
AC22G(M)	46.0
AC22G	50.0
AC32G	55.5

Table 4
Parameters of macro-texture Gompertz modified model.

Parameter	a_1	a_2	a_3	a_4
Value	1.3483	380.25	0.1249	0.0046
Standard error	0.0428	78.208	0.0049	0.0001
t-Statistic	31.438	4.8620	25.362	39.493
Pr (>|t|)	<2e−16	2.70e−06	<2e−16	<2e−16

Table 5
Parameters of macro-texture cubic polynomial model.

Parameter	a_1	a_2	a_3
Value	1.719e−05	7.614e−04	1.137e−02
Standard error	1.204e−06	1.050e−04	2.229e−03
t-Statistic	14.279	7.250	5.102
Pr (>|t|)	<2e−16	1.53e−11	9.15e−07

Table 6
Parameters of macro-texture exponential model.

Parameter	a_1	a_2	a_3
Value	0.5055	6.2044	0.1320
Standard error	0.0233	0.1568	0.0039
t-Statistic	21.66	39.55	33.67
Pr (>|t|)	<2e−16	<2e−16	<2e−16

Table 7
Goodness of fit for the macro-texture predictive models.

Model	RMSE
Gompertz modified	0.0247
Cubic polynomial	0.0454
Exponential	0.0399

Table 8
Model parameters for dosage of 125 g/m².

Parameter	Value	Standard error	*t*-Statistic	Pr (>|t|)
a_1	6835.6	21.369	319.888	<2e−16
a_2	87.386	4.1481	21.066	<2e−16
a_3	6.1092	0.2156	28.338	<2e−16
a_4	0.1332	0.0032	42.109	<2e−16
a_5	21223	466.80	45.466	<2e−16
a_6	8761.8	1247.2	7.0251	5.9e−12
a_7	0.1648	0.0028	57.870	<2e−16

Table 9
Model parameters for dosage of 250 g/m².

Parameter	Value	Standard error	*t*-Statistic	Pr (>|t|)
a_1	6533.1	38.389	170.182	<2e−16
a_2	123.63	7.2441	17.067	<2e−16
a_3	7.8934	0.3661	21.561	<2e−16
a_4	0.1546	0.0052	29.599	<2e−16
a_5	21223	688.30	27.176	<2e−16
a_6	18705	9265.4	3.3163	9.7e−4
a_7	0.1880	0.0059	31.646	<2e−16

Table 10
Model parameters for dosage of 375 g/m².

Parameter	Value	Standard error	*t*-Statistic	Pr (>|t|)
a_1	6549.8	15.819	414.04	<2e−16
a_2	87.621	3.0950	28.310	<2e−16
a_3	4.4926	0.1621	27.714	<2e−16
a_4	0.0990	0.0024	41.288	<2e−16
a_5	16713	355.57	47.004	<2e−16
a_6	6921.1	908.34	7.6195	1.0e−13
a_7	0.1607	0.0026	60.958	<2e−16

Table 11
Model parameters for dosage of 500 g/m².

Parameter	Value	Standard error	*t*-Statistic	Pr (>|t|)
a_1	6769.0	9.4057	719.74	<2e−16
a_2	61.749	1.8387	33.584	<2e−16
a_3	2.8376	0.0962	29.491	<2e−16
a_4	0.0628	0.0014	44.206	<2e−16
a_5	10557	214.42	49.236	<2e−16
a_6	6810.5	849.84	8.0138	5.9e−15
a_7	0.1602	0.0025	63.922	<2e−16

Table 12
Root Mean Square Error (*RMSE*) for the dosage models.

Dosage [g/m²]	RMSE
125	789.75
250	928.00
375	608.90
500	680.64

Table 13
Shear strength estimative models based on emulsion dosages.

Dosage [g/m²]	Shear strength estimative model
125	$R = 6835.6 + 87.386 * G - 6.1092 * G^2 + 0.1332 * G^3 - 21223 * e^{(-8761.8e^{(-0.1648*G)})}$
250	$R = 6533.1 + 123.63 * G - 7.8934 * G^2 + 0.1546 * G^3 - 18705 * e^{(-30727e^{(-0.1880*G)})}$
375	$R = 6549.8 + 87.621 * G - 4.4926 * G^2 + 0.0990 * G^3 - 16713 * e^{(-6921.1e^{(-0.1607*G)})}$
500	$R = 6769.7 + 61.749 * G - 2.8376 * G^2 + 0.0628 * G^3 - 10557 * e^{(-6810.5e^{(-0.1602*G)})}$

Table 14
Absorption model parameters for 250 g/m².

Parameter	Value	Standard error	*t*-Statistic	Pr (>|t|)
a_1	59.839	4.348	13.762	<2e−16
a_2	0.212	0.033	6.358	1.00e−07
a_3	−10.114	1.566	−6.459	7.13e−08
a_4	29.728	2.862	10.386	2.05e−13

Table 15
Absorption model parameters for 375 g/m².

Parameter	Value	Standard error	*t*-Statistic	Pr (>|t|)
a_1	43.167	4.312	10.011	6.45e−13
a_2	0.191	0.040	4.816	1.77e−05
a_3	−9.391	1.929	−4.867	1.49e−05
a_4	48.251	3.008	16.042	<2e−16

Table 16
Absorption model parameters for 500 g/m².

Parameter	Value	Standard error	*t*-Statistic	Pr (>|t|)
a_1	41.639	3.954	10.531	1.32e−13
a_2	0.341	0.087	3.927	3.00e−04
a_3	−16.657	4.201	−3.965	2.67e−04
a_4	49.626	2.642	17.787	<2e−16

Table 17
Goodness of fit for the absorption models.

Dosage [g/m²]	RMSE
250	14.7458
375	11.6065
500	12.0964